

# Chemisorption sites of CO on small gold clusters and transitions from chemisorption to physisorption

Hua-Jin Zhai and Lai-Sheng Wang<sup>a)</sup>

*Department of Physics, Washington State University, Richland, Washington 99352  
and W. R. Wiley Environmental Molecular Sciences Laboratory, Pacific Northwest National Laboratory,  
MS K8-88, P.O. Box 999, Richland, Washington 99352*

(Received 4 November 2004; accepted 30 November 2004; published online 18 January 2005)

Gold clusters adsorbed with CO,  $\text{Au}_m(\text{CO})_n^-$  ( $m=2-5$ ;  $n=0-7$ ), were studied by photoelectron spectroscopy (PES). The first few CO adsorptions were observed to induce significant redshifts to the PES spectra relative to pure gold clusters. For each Au cluster, a critical CO number ( $n_c$ ) was observed, beyond which the PES spectra of  $\text{Au}_m(\text{CO})_n^-$  change very little with increasing  $n$ .  $n_c$  was shown to correspond exactly to the available low coordination apex sites in each Au cluster. CO first chemisorbs to these sites and additional CO then only physisorbs to the chemisorption-saturated  $\text{Au}_m(\text{CO})_n^-$  complexes. © 2005 American Institute of Physics. [DOI: 10.1063/1.1850091]

Gold is the noblest of all metals in the periodic table. Therefore, the discovery of catalytic activity in gold nanoparticles<sup>1</sup> was quite remarkable and has attracted considerable attention in nanocatalysis and cluster science.<sup>2-33</sup> In particular, gold nanoparticles are able to catalyze low temperature CO oxidation, whose mechanisms have been the focus of extensive investigations lately.<sup>3-13</sup> Different models have been proposed, but the exact mechanisms that govern this highly useful catalytic reaction are still under debate.<sup>34</sup> Size-selected cluster deposition studies<sup>11,12</sup> and gas phase experimental<sup>14-23</sup> and theoretical<sup>24-29</sup> studies represent alternative approaches to model this reaction in a well-controlled manner and can provide fundamental understanding at the molecular level. Recent experimental and theoretical studies established that  $\text{O}_2$  adsorbs molecularly on gold clusters and nanoparticles.<sup>6,14,25,26,29</sup> Co-adsorption of CO and  $\text{O}_2$  on small gold clusters was also investigated by mass-spectrometry-based experiments and by DFT calculations.<sup>16-18,28</sup> Importantly, they were shown to adsorb cooperatively, rather than competitively.<sup>16,18</sup> However, relatively little experimental information is available on how CO interacts with small gold clusters and nanoparticles, particularly regarding the electronic and structural properties of the CO chemisorbed gold clusters. A number of chemical reaction studies of gold clusters with CO have been reported and size dependence and saturation were observed.<sup>19-22</sup> There have also been recent experimental and theoretical works concerning CO adsorption on isolated and supported gold clusters,<sup>4,8,27,28</sup> but definitive experimental structural information is still elusive.

Here we report a photoelectron spectroscopy (PES) study of CO-adsorbed gold clusters,  $\text{Au}_m(\text{CO})_n^-$  ( $m=2-5$ ;  $n=0-7$ ). We observed that the first few CO induce significant shifts to the PES spectra relative to those of the bare clusters, suggesting strong chemisorption interactions between CO and the gold clusters. For each series, the CO

adsorption reaches a critical number ( $n_c$ ), beyond which the PES spectra change very little with increasing  $n$ , a clear spectroscopic signature of a transition from chemi- to physisorption. The critical CO numbers,  $n_c$ , are 2, 2, 3, and 4 for  $\text{Au}_m^-$  ( $m=2-5$ ), respectively, corresponding exactly to the available low coordination apex sites on the respective clusters: the two terminal Au atoms for the linear  $\text{Au}_2^-$  and  $\text{Au}_3^-$ , the outer three Au atoms on the Y-shaped  $\text{Au}_4^-$ , and the four outer Au atoms on the planar M-shaped  $\text{C}_{2v}\text{Au}_5^-$ . With the exception of  $\text{Au}_5\text{CO}^-$ , the CO adsorption in the chemisorption regime induces significant decreases to the electron binding energies of the chemisorbed clusters. The reduction of electron binding energies upon CO chemisorption enhances  $\text{O}_2$  adsorption, which requires an electron transfer from the cluster to  $\text{O}_2$ . Thus the current observation also provides the electronic and spectroscopic basis for the cooperative chemisorption of CO and  $\text{O}_2$  on gold clusters and may be important to elucidate the catalytic mechanisms of gold nanoparticles.

The experiments were carried out using a magnetic bottle PES apparatus equipped with a laser vaporization cluster source, details of which were described elsewhere.<sup>35</sup> Briefly, the  $\text{Au}_m(\text{CO})_n^-$  cluster anions were produced by laser vaporization of a pure gold target in the presence of a helium carrier gas seeded with 2% CO. Various  $\text{Au}_m(\text{CO})_n^-$  clusters were generated and mass-analyzed using a time-of-flight mass spectrometer. The  $\text{Au}_m(\text{CO})_n^-$  ( $m=2-5$ ;  $n=0-7$ ) species of current interest<sup>36</sup> were each mass-selected and decelerated before being photodetached. Four detachment photon energies were used in the current study: 532 nm (2.331 eV), 355 nm (3.496 eV), 266 nm (4.661 eV), and 193 nm (6.424 eV). Photoelectrons were collected at nearly 100% efficiency by the magnetic bottle and analyzed in a 3.5 m long electron flight tube. The PES spectra were calibrated using the known spectra of  $\text{Au}^-$  and  $\text{Rh}^-$ , and the energy resolution of the apparatus was  $\Delta E_k/E_k \sim 2.5\%$ , that is,  $\sim 25$  meV for 1 eV electrons.

<sup>a)</sup>Electronic mail: ls.wang@pnl.gov

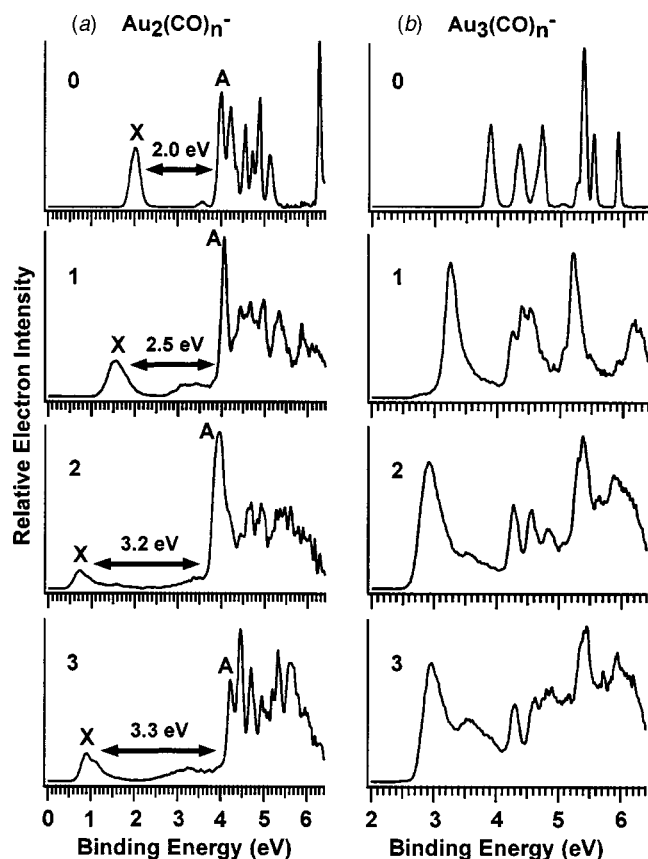


FIG. 1. Photoelectron spectra of (a)  $\text{Au}_2(\text{CO})_n^-$  and (b)  $\text{Au}_3(\text{CO})_n^-$  at 193 nm (6.424 eV) for  $n=0-3$ . Energy gaps between features X and A for each species are labeled in (a).

The 193 nm PES spectra of  $\text{Au}_2(\text{CO})_n^-$  and  $\text{Au}_3(\text{CO})_n^-$  with  $n$  up to 3 are shown in Fig. 1 and those for chemisorbed  $\text{Au}_4^-$  and  $\text{Au}_5^-$  are shown in Fig. 2 with  $n$  up to 5. Data were obtained for  $\text{Au}_3^-$  up to  $n=5$  and for  $\text{Au}_4^-$  and  $\text{Au}_5^-$  up to  $n=7$ . But the additional spectra do not show significant changes and are not shown. Spectra for all the clusters were taken at four different detachment energies (532, 355, 266, and 193 nm). The higher photon energies allow more electronic transitions to be accessed, whereas the lower photon energies are able to provide better-resolved spectra for the lower binding energy features. The adiabatic (ADE) and vertical (VDE) detachment energies for the lowest binding energy feature were obtained from the low photon energy spectra and are given in Table I for all species. The ADEs are also plotted in Fig. 3 as a function of CO numbers.

$\text{Au}_2$  is closed shell with a large HOMO-LUMO gap (2.0 eV), as revealed in the PES spectrum of  $\text{Au}_2^-$  [Fig. 1(a)]. Upon CO adsorption, the spectral features are similar to those of  $\text{Au}_2^-$ , but the lowest binding energy feature (X) is significantly redshifted by 0.69 eV for the first CO and 0.56 eV by the second CO. However, the third CO does not produce a redshift, but rather induces a slight blueshift by 0.17 eV (Table I). For  $\text{Au}_3^-$ , we also observed that the first two CO induce significant redshift to the PES spectra [Fig. 1(b)], whereas the third CO appears to have very little effect: it produces a very slight blueshift (0.04 eV), but the spectral pattern of  $\text{Au}_3(\text{CO})_3^-$  is nearly identical to that of

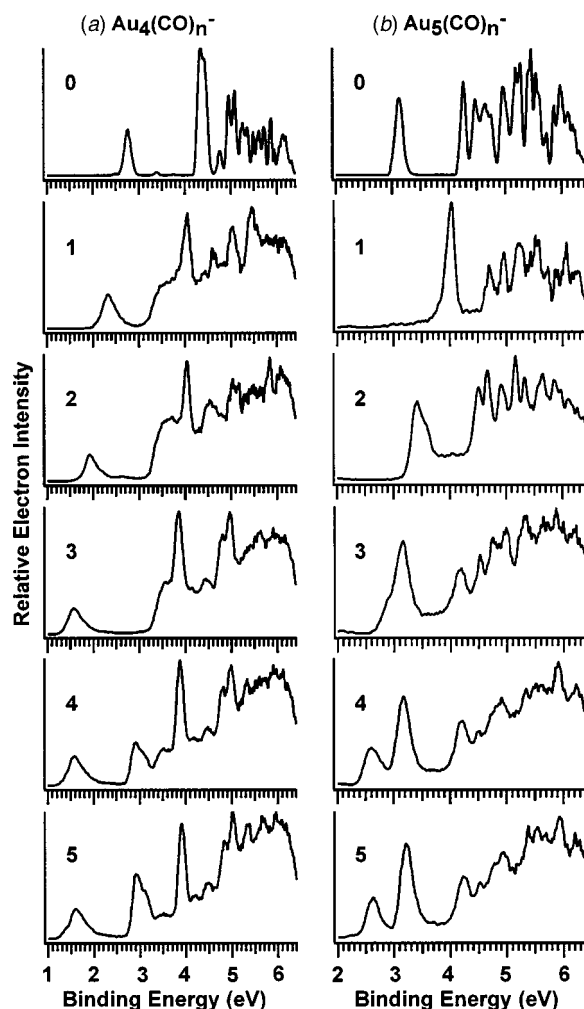


FIG. 2. Photoelectron spectra of (a)  $\text{Au}_4(\text{CO})_n^-$  and (b)  $\text{Au}_5(\text{CO})_n^-$  at 193 nm (6.424 eV) for  $n=0-5$ .

$\text{Au}_3(\text{CO})_2^-$ . We have PES data up to  $n=5$ , but the spectra of  $\text{Au}_3(\text{CO})_4^-$  and  $\text{Au}_3(\text{CO})_5^-$  (not shown) are identical to that of  $\text{Au}_3(\text{CO})_3^-$ , each with a very small blueshift (Table I). The CO adsorption behavior of  $\text{Au}_4^-$  is similar, but here the first three CO each induce a significant redshift to the PES spectra [Fig. 2(a)]. The fourth CO only produces a redshift of 0.02 eV. Additional CO up to  $n=7$  yielded PES spectra identical to that of  $\text{Au}_3(\text{CO})_4^-$ , as can be seen by the similarity between the spectra of  $n=4$  and 5 in Fig. 2(a). The CO adsorption behavior of  $\text{Au}_5^-$  is slightly different, only because the first CO induces a huge blueshift of 0.85 eV [Fig. 2(b)]. This is due to the special electronic structure of  $\text{Au}_5(\text{CO})^-$ , which can be considered to be a eight-electron system (a major shell closing in the electron shell model) as discussed previously.<sup>19-21,37</sup> However, subsequent CO adsorption each produces redshift up to  $n=4$ , beyond which both the electron binding energies and the spectral pattern change little between  $n=5$  to 7. Starting at  $\text{Au}_5(\text{CO})_3^-$ , the first PES band seemed to show a splitting, which can be seen more clearly in  $\text{Au}_5(\text{CO})_4^-$  and all the large clusters for  $n=5-7$ .<sup>38</sup>

Our experimental observation suggests that the first few CO interact more strongly with the  $\text{Au}_m^-$  clusters,<sup>39</sup> inducing

TABLE I. Observed adiabatic (ADE) and vertical (VDE) detachment energies from the photoelectron spectra of  $Au_m(CO)_n^-$  ( $m=2-5$ ;  $n=0-7$ ).

Species	ADE (eV) <sup>a</sup>	$\Delta$ ADE (eV) <sup>b</sup>	VDE (eV) <sup>a</sup>
$Au_2^-$	1.94 (2)		2.01 (2)
$Au_2(CO)^-$	1.25 (5)	-0.69	1.50 (3)
$Au_2(CO)_2^-$	0.69 (5)	-0.56	0.69 (3)
$Au_2(CO)_3^-$	0.86 (3)	0.17	0.86 (3)
$Au_3^-$	3.88 (2)		3.88 (2)
$Au_3(CO)^-$	3.20 (3)	-0.68	3.25 (3)
$Au_3(CO)_2^-$	2.73 (3)	-0.47	2.90 (3)
$Au_3(CO)_3^-$	2.77 (3)	0.04	2.94 (3)
$Au_3(CO)_4^-$	2.80 (3)	0.03	2.99 (3)
$Au_3(CO)_5^-$	2.85 (3)	0.05	3.03 (3)
$Au_4^-$	2.70 (2)		2.77 (2)
$Au_4(CO)^-$	2.12 (5)	-0.58	2.38 (3)
$Au_4(CO)_2^-$	1.77 (5)	-0.35	1.95 (2)
$Au_4(CO)_3^-$	1.32 (2)	-0.45	1.35 (2)
$Au_4(CO)_4^-$	1.30 (2)	-0.02	1.34 (2)
$Au_4(CO)_5^-$	1.33 (2)	0.03	1.36 (2)
$Au_4(CO)_6^-$	1.35 (2)	0.02	1.38 (2)
$Au_4(CO)_7^-$	1.37 (2)	0.02	1.41 (2)
$Au_5^-$	3.06 (3)		3.11 (3)
$Au_5(CO)^-$	3.91 (5)	0.85	4.02 (3)
$Au_5(CO)_2^-$	3.32 (5)	-0.59	3.41 (3)
$Au_5(CO)_3^-$	2.68 (5)	-0.64	2.91 (3)
$Au_5(CO)_4^-$	2.42 (3)	-0.26	2.58 (3)
$Au_5(CO)_5^-$	2.43 (3)	0.01	2.60 (3)
$Au_5(CO)_6^-$	2.45 (3)	0.02	2.63 (3)
$Au_5(CO)_7^-$	2.49 (3)	0.04	2.66 (3)

<sup>a</sup>Numbers in parentheses represent experimental uncertainties in the last digit.

<sup>b</sup> $\Delta$ ADE $\equiv$ ADE[ $Au_m(CO)_n^-$ ] - ADE[ $Au_m(CO)_{n-1}^-$ ], which characterizes the contribution of the  $n$ th CO molecule to the electron binding energy of  $Au_m(CO)_n^-$ .

significant redshift to the electron binding energy and representing chemisorption. Once the available sites on the  $Au_m^-$  clusters are used up, further CO adsorption has relatively little effect on the electronic structure of the chemisorbed  $Au_m(CO)_n^-$  clusters, indicating the physisorption regime. Thus, the PES spectra (Figs. 1 and 2) reveal vividly a transition from chemi- to physisorption of CO on Au clusters. Importantly, the maximum numbers of chemisorbed CO correspond precisely to the available low-coordination apex sites on each  $Au_m^-$  cluster, as can be seen from the structures of the bare Au clusters given in Fig. 3.<sup>30-32</sup> The letters (a,b,c,d) indicate the CO chemisorption sites. For  $Au_2^-$  and  $Au_3^-$ , the two terminal Au atoms (a,b) should be the natural sites for CO chemisorption. For  $Au_4^-$ , there are two low-lying isomers, a linear one and a Y-shaped one.<sup>30-32</sup> The maximum of three chemisorbed CO suggests that the  $Au_4^-$  cluster possesses the Y-shaped structure,<sup>31,32</sup> which has three peripheral low-coordination sites. The most likely chemisorption sites for the M-shaped  $Au_5^-$  are also labeled in Fig. 3. It is interesting to note that the fifth Au atom with a coordination number of only 4 is not a chemisorption site. The current experimental observation is consistent with a recent theoretical study of multiple CO adsorption on small Au cluster anions,<sup>28</sup> as well as recent experimental and theoretical evidence that shows that the active sites for CO adsorption on supported Au nanoparticles are in fact low-coordination Au atoms.<sup>8,13</sup> In the tetrahedral  $Au_{20}$  cluster,<sup>33</sup>

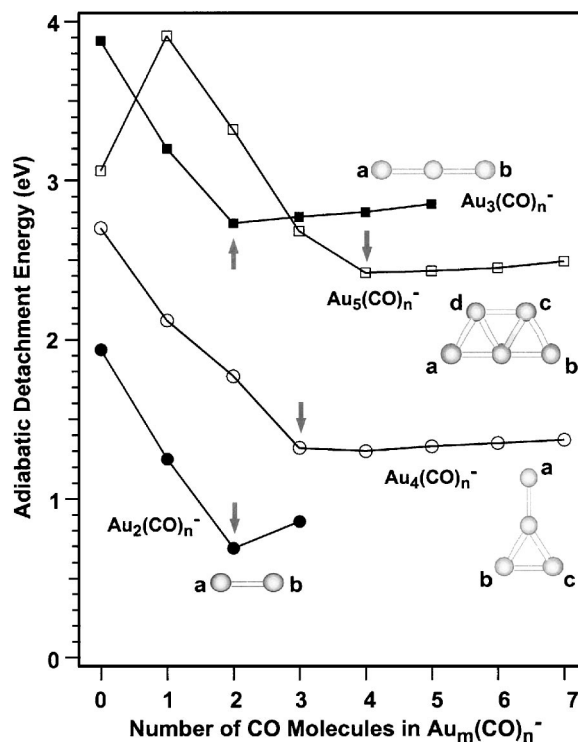


FIG. 3. Adiabatic electron detachment energies of the  $Au_m(CO)_n^-$  complexes versus the numbers of CO. The arrows indicate the transition from chemisorption to physisorption, i.e., the critical CO numbers beyond which further CO adsorptions do not change the adiabatic detachment energies and spectral pattern significantly. Schematic structures of the  $Au_m^-$  ( $m=2-5$ ) cluster anions (Refs. 30-32) are also shown, where the letters a, b, c, and d label the active sites for CO chemisorption.

DFT calculations show that the four corner atoms are the favorite sites for CO adsorption with a 0.84 eV CO binding energy, whereas the four face-center atoms are the least favorite with a CO binding energy of only 0.15 eV.

The PES data also provides insight into the mechanisms for the cooperative coadsorption of CO and  $O_2$  on gold cluster anions.<sup>16,18</sup> The interactions of Au clusters with CO and  $O_2$  are fundamentally different. CO interacts with Au as a  $\sigma$  electron donor, whereas  $O_2$  is an electron acceptor. We note that the CO chemisorption induces significant lowering of the electron binding energies to the  $Au_m(CO)_n^-$  chemisorbed clusters, making them better electron donors and enhancing their interaction with  $O_2$ . The chemisorption of  $O_2$  withdraws electron density from Au clusters, making them better electron acceptors and enhancing their interactions with CO. Thus, CO and  $O_2$  are chemisorption promoters to each other, naturally leading to cooperative adsorption on Au clusters. The same mechanism should work in real gold catalysts and may hold the key for understanding why gold nanoparticles are capable of catalyzing CO oxidation at low temperatures.

This work was supported by the National Science Foundation (CHE-0349426) and performed at the EMSL, a national scientific user facility sponsored by DOE's Office of Biological and Environmental Research and located at the Pacific Northwest National Laboratory, operated for DOE by Battelle.

- <sup>1</sup>M. Haruta, *Catal. Today* **36**, 153 (1997) and references therein.
- <sup>2</sup>G. C. Bond and D. T. Thompson, *Catal. Rev. - Sci. Eng.* **41**, 319 (1999).
- <sup>3</sup>M. Valden, X. Lai, and D. W. Goodman, *Science* **281**, 1647 (1998).
- <sup>4</sup>D. C. Meier and D. W. Goodman, *J. Am. Chem. Soc.* **126**, 1892 (2004).
- <sup>5</sup>T. S. Kim, J. D. Stiehl, C. T. Reeves, R. J. Meyer, and C. B. Mullins, *J. Am. Chem. Soc.* **125**, 2018 (2003).
- <sup>6</sup>J. D. Stiehl, T. S. Kim, S. M. McClure, and C. B. Mullins, *J. Am. Chem. Soc.* **126**, 1606 (2004).
- <sup>7</sup>J. Guzman and B. C. Gates, *J. Am. Chem. Soc.* **126**, 2672 (2004).
- <sup>8</sup>C. Lemire, R. Meyer, S. Shaikhutdinov, and H. J. Freund, *Angew. Chem., Int. Ed. Engl.* **43**, 118 (2004).
- <sup>9</sup>Z. P. Liu, P. Hu, and A. Alavi, *J. Am. Chem. Soc.* **124**, 14770 (2002).
- <sup>10</sup>L. M. Molina and B. Hammer, *Phys. Rev. Lett.* **90**, 206102 (2003).
- <sup>11</sup>A. Sanchez, S. Abbet, U. Heiz, W. D. Schneider, H. Hakkinen, R. N. Barnett, and U. Landman, *J. Phys. Chem. A* **103**, 9573 (1999).
- <sup>12</sup>S. Lee, C. Fan, T. Wu, and S. L. Anderson, *J. Am. Chem. Soc.* **126**, 5682 (2004).
- <sup>13</sup>N. Lopez, T. V. W. Janssens, B. S. Clausen, Y. Xu, M. Mavrikakis, T. Bligaard, and J. K. Nørskov, *J. Catal.* **223**, 232 (2004).
- <sup>14</sup>D. Stolcic, M. Fischer, G. Gantefor, Y. D. Kim, Q. Sun, and P. Jena, *J. Am. Chem. Soc.* **125**, 2848 (2003).
- <sup>15</sup>M. L. Kimble, A. W. Castleman, Jr., R. Mitric, C. Burgel, and V. Bonacic-Koutecky, *J. Am. Chem. Soc.* **126**, 2526 (2004).
- <sup>16</sup>J. Hagen, L. D. Socaciu, U. Heiz, T. M. Bernhardt, and L. Woste, *Eur. Phys. J. D* **24**, 327 (2003).
- <sup>17</sup>L. D. Socaciu, J. Hagen, T. M. Bernhardt, L. Woste, U. Heiz, H. Hakkinen, and U. Landman, *J. Am. Chem. Soc.* **125**, 10437 (2003).
- <sup>18</sup>W. T. Wallace and R. L. Whetten, *J. Am. Chem. Soc.* **124**, 7499 (2002).
- <sup>19</sup>M. A. Nygren, P. E. M. Siegbahn, C. Jin, T. Guo, and R. E. Smalley, *J. Chem. Phys.* **95**, 6181 (1991).
- <sup>20</sup>T. H. Lee and K. M. Ervin, *J. Phys. Chem.* **98**, 10023 (1994).
- <sup>21</sup>W. T. Wallace and R. L. Whetten, *J. Phys. Chem. B* **104**, 10964 (2000).
- <sup>22</sup>I. Balteanu, O. P. Balaj, B. S. Fox, M. K. Beyer, Z. Bastl, and V. E. Bondybey, *Phys. Chem. Chem. Phys.* **5**, 1213 (2003).
- <sup>23</sup>G. Luttgens, N. Pontius, P. S. Bechthold, M. Neeb, and W. Eberhardt, *Phys. Rev. Lett.* **88**, 076102 (2002).
- <sup>24</sup>B. Yoon, H. Hakkinen, and U. Landman, *J. Phys. Chem. A* **107**, 4066 (2003).
- <sup>25</sup>S. A. Varganov, R. M. Olson, M. S. Gordon, and H. Meitu, *J. Chem. Phys.* **119**, 2531 (2003).
- <sup>26</sup>X. Ding, Z. Li, J. Yang, J. G. Hou, and Q. Zhu, *J. Chem. Phys.* **120**, 9594 (2004).
- <sup>27</sup>X. Wu, L. Senapati, S. K. Nayak, A. Selloni, and M. Hajaligol, *J. Chem. Phys.* **117**, 4010 (2002).
- <sup>28</sup>D. W. Yuan and Z. Zeng, *J. Chem. Phys.* **120**, 6574 (2004).
- <sup>29</sup>H. Hakkinen and U. Landman, *J. Am. Chem. Soc.* **123**, 9704 (2001).
- <sup>30</sup>H. Hakkinen and U. Landman, *Phys. Rev. B* **62**, R2287 (2000).
- <sup>31</sup>F. Furche, R. Ahlrichs, P. Weis, C. Jacob, S. Gilb, T. Bierweiler, and M. M. Kappes, *J. Chem. Phys.* **117**, 6982 (2002).
- <sup>32</sup>H. Hakkinen, B. Yoon, U. Landman, X. Li, H. J. Zhai, and L. S. Wang, *J. Phys. Chem. A* **107**, 6168 (2003).
- <sup>33</sup>J. Li, X. Li, H. J. Zhai, and L. S. Wang, *Science* **299**, 864 (2003).
- <sup>34</sup>A. Cho, *Science* **299**, 1684 (2003).
- <sup>35</sup>L. S. Wang, H. S. Cheng, and J. Fan, *J. Phys. Chem.* **102**, 9480 (1995).
- <sup>36</sup>For larger clusters it became difficult to obtain systematic and clean data because of a near mass degeneracy between 7 CO (mass: 196) and Au (mass: 197). For example,  $\text{Au}_5(\text{CO})_8^-$  would interfere with  $\text{Au}_6(\text{CO})^-$ , although experimental conditions can be tuned to minimize the interference.
- <sup>37</sup>Similarly  $\text{Au}_3(\text{CO})_2^-$  can be considered as an eight electron system. Even though the photoelectron spectrum of  $\text{Au}_3(\text{CO})_2^-$  did not exhibit any special features, a previous reaction kinetic study between  $\text{Au}_3^-$  and CO (Ref. 16) revealed that  $\text{Au}_3(\text{CO})_2^-$  is particularly stable.
- <sup>38</sup>This splitting could be due to either structural isomers or new electronic features induced by CO chemisorption. A firm interpretation would require detailed theoretical calculations.
- <sup>39</sup>Preliminary PES data have been obtained for  $\text{Au}_m(\text{CO})_n^-$  with  $m=6-8$  and  $n=4-6$ . Although saturation was not observed, the redshift of the electron binding energy upon CO chemisorption was observed in each case.